Polaron formation: Ehrenfest dynamics vs. exact results

Guangqi Li, Bijan Movaghar, Abraham Nitzan, and Mark A. Ratner

Citation: The Journal of Chemical Physics **138**, 044112 (2013); doi: 10.1063/1.4776230
View online: http://dx.doi.org/10.1063/1.4776230
View Table of Contents: http://scitation.aip.org/content/aip/journal/jcp/138/4?ver=pdfcov
Published by the AIP Publishing

Polaron formation: Ehrenfest dynamics vs. exact results

Guangqi Li,[1] Bijan Movaghar,[1] Abraham Nitzan,[2,a)] and Mark A. Ratner[1,b)]
[1]*Department of Chemistry, Northwestern University, Evanston, Illinois 60208, USA*
[2]*School of Chemistry, Tel-Aviv University, Tel-Aviv 69978, Israel*

(Received 30 October 2012; accepted 31 December 2012; published online 31 January 2013)

We use a one-dimensional tight binding model with an impurity site characterized by electron-vibration coupling, to describe electron transfer and localization at zero temperature, aiming to examine the process of polaron formation in this system. In particular we focus on comparing a semiclassical approach that describes nuclear motion in this many vibronic-states system on the Ehrenfest dynamics level to a numerically exact fully quantum calculation based on the Bonca-Trugman method [J. Bonča and S. A. Trugman, Phys. Rev. Lett. **75**, 2566 (1995)]. In both approaches, thermal relaxation in the nuclear subspace is implemented in equivalent approximate ways: In the Ehrenfest calculation the uncoupled (to the electronic subsystem) motion of the classical (harmonic) oscillator is simply damped as would be implied by coupling to a Markovian zero temperature bath. In the quantum calculation, thermal relaxation is implemented by augmenting the Liouville equation for the oscillator density matrix with kinetic terms that account for the same relaxation. In both cases we calculate the probability to trap the electron by forming a polaron and the probability that it escapes to infinity. Comparing these calculations, we find that while both result in similar long time yields for these processes, the Ehrenfest-dynamics based calculation fails to account for the correct time scale for the polaron formation. This failure results, as usual, from the fact that at the early stage of polaron formation the classical nuclear dynamics takes place on an unphysical average potential surface that reflects the distributed electronic population in the system, while the quantum calculation accounts fully for correlations between the electronic and vibrational subsystems. © *2013 American Institute of Physics*. [http://dx.doi.org/10.1063/1.4776230]

I. INTRODUCTION

Electron transfer between molecular systems has long been recognized as a key process in many research fields of chemistry, physics, and biology.[1–5] Many of its aspects are described by the Marcus theory,[6] which has been extended to describe such areas as artificial solar-energy conversion[7–9] and molecular electronics.[10–17]

The Marcus theory relies in an essential way on electron-vibration interaction. The initial and final states of the electron transfer process are fully equilibrated polarons localized on different sites, and transitions between them are evaluated within the assumptions of transition state theory. Motion in an extended system is assumed to be a succession of hopping steps, each described as a Marcus process. In the other extreme limit, electronic motion in a frozen lattice, the electron moves within its energy band, most simply described using a tight binding model. In between these limits, electron-phonon interaction and band motion can change the electron's character from being weakly perturbed by electron-phonon scattering to polaronic motion whose discrete representation is the succession of hopping processes described above.

In the present paper we are interested in situations where electronic band motion competes on the same time scale with polaron formation, so that the dynamics of the latter process has to be considered explicitly. Such considerations are relevant to recently studied models of photovoltaic cells,[18,19] where electrons (or holes) are injected at some location in the system and a useful process is defined by their absorption at another (e.g., an electrode surface). The yield of such processes, determined by the competition between electronic motion and loss processes[19] (e.g., carrier recombination) is expected to be sensitive to electron-phonon interactions, and in particular to transient polaron formation.

Exact treatment of such coupled many-body systems is difficult, and it is tempting to resort to approximations such as the semiclassical mean field (Ehrenfest) dynamics. In this approximation the electronic wavefunction $\Psi(r, t)$ (r represents the electronic coordinates and t is the time) evolves under a time-dependent Hamiltonian defined by a classical nuclear trajectory, schematically represented by a nuclear coordinate $R(t)$, while the latter is obtained by solving the Newton equation for the nuclear motion with a potential in which the vibronic coupling $V(r, R)$ is replaced by its instantaneous expectation value $V(R, t) = \langle\Psi(r, t)|V(r, R)|\Psi(r, t)\rangle$. Such an approximation, essentially a dynamical extension of the Born-Oppenheimer (BO) approximation, is expected to perform well when the electronic motion is fast, throughout the relevant electronic subspace, relative to the nuclear dynamics. Its failure in describing processes in which transitions between BO electronic adiabatic states take place on the same time scale as nuclear motions is also well known. Indeed, in the analogous case of electron solvation in polar liquids such

a)nitzan@post.tau.ac.il.
b)ratner@northwestern.edu.

non-adiabatic processes have been addressed with the necessary accounting for the quantum nature of the nuclear motion,[20–22] usually within the surface hopping methodology.[21–23] Still, because Ehrenfest dynamics is so easy to implement and to use, it is of interest to assess its performance as an approximation to exact results in the context described above.[24] This is the purpose of the present paper. Using a model that is simple enough to solve up to any desired level of accuracy, we focus on two observables: the extent of the polaronic localization and its formation time, and compare results obtained from the semiclassical Ehrenfest dynamics approach to the exact, fully quantum, results. For model parameters that support polaron formation we find that, while the Ehrenfest calculation yields a similar final state as the exact one, it predicts a polaron formation time that is an order of magnitude longer than the exact result. This implies that Ehrenfest dynamics cannot be used as a reliable tool for assessing polaronic effects in such systems. This does not exclude its possible applicability in larger systems at higher temperatures with many more nuclear degrees of freedom, but indicates that its use should be exercised with caution and after performing suitable benchmark calculations.

We start by formulating the basic Hamiltonian model and comparing the different predictions of the quantum and the semiclassical descriptions in Sec. II. In Sec. III we define the population operator and the population formation time. Numerical calculation and discussions are given in Secs. IV and V, and a conclusion follows.

II. THEORETICAL MODEL

We consider an $n+1$-site tight-binding electron model (below we take $n=4$) coupled to a system of harmonic oscillators (see Fig. 1). We assume that only one oscillator (henceforth referred to as the "primary" vibration) directly couples to the electronic systems. The others ("secondary" phonons) constitute a thermal bath that affects relaxation in the primary system. The Hamiltonian of the whole system shown is

$$H = H_S + H_B + H_{SB}, \tag{1}$$

$$H_S = \sum_{l=0}^{4} \varepsilon_l c_l^\dagger c_l + V \sum_{l=0}^{3} (c_l^\dagger c_{l+1} + c_{l+1}^\dagger c_l) + \hbar\omega_0 d_0^\dagger d_0 + \alpha_2 c_2^\dagger c_2 (d_0^\dagger + d_0), \tag{2}$$

$$H_B = \sum_{s=1}^{\infty} \hbar\omega_s d_s^\dagger d_s, \tag{3}$$

$$H_{SB} = \sum_{s=1}^{\infty} \lambda_s (d_0^\dagger d_s + d_s^\dagger d_0). \tag{4}$$

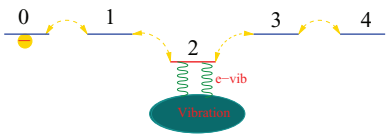

FIG. 1. The model chain including 5 sites. The electron-vibration interaction is associated with transitions into and out of the middle site 2.

Here H_S corresponds to the electronic system (described by the creation and annihilation operators for each site l, $c_l^\dagger$, c_l), together with the primary vibration, of frequency ω_0 described by the creation and annihilation operators $d_0^\dagger$, d_0. H_B describes the secondary phonon bath ($d_s^\dagger$, d_s are the creation and annihilation operators for phonon of frequency ω_s) and H_{SB} is the coupling between the primary vibration and secondary phonons. ε_l is the on-site energy level of site l, V is the coupling parameter associated with electron tunneling between nearest neighbor sites. The parameters α_2 and λ_s characterize to the coupling between the electronic state at site 2 and the primary vibration, and between the primary vibration and secondary phonons, respectively.

A. The quantum approach

In the quantum approach, the evolution described by the Hamiltonian (2) is treated essentially exactly,[24] using the basis set $\{|n, \nu>\}$ where n and ν denote the electronic state localized on site n and the vibrational state ν of the primary oscillator. In the numerical calculation we truncate the set $\{\nu\}$ at some value, $\nu_{\max}$ and test for convergence as $\nu_{\max}$ increases.

The coupling to the thermal bath is treated in the master equation approach: The density matrix ρ_T of the whole system is assumed to keep the form $\rho_T = \rho_S \otimes \rho_B$, where ρ_B, the density matrix of the thermal bath (secondary phonons), is assumed to remain in equilibrium at the ambient temperature. Then the quantum master equation for ρ_S is

$$i\hbar \frac{\partial \rho_S(t)}{\partial t} = [H_S, \rho_S(t)] - i\hbar\gamma_0 [d_0^\dagger d_0 \rho_S(t) + \rho_S(t) d_0^\dagger d_0 - 2 d_0 \rho_S(t) d_0^\dagger]/2, \tag{5}$$

where γ_0 is the vibrational relaxation rate induced by the vibration-phonon bath coupling. It is equal to the imaginary part of the vibration self-energy Σ given by

$$\gamma_0(\omega)/2 = \frac{1}{\hbar} \mathrm{Im}\{\Sigma_{\mathrm{vibration}}(\omega)\} = \frac{1}{\hbar} \sum_{\mathrm{s}} |\lambda_{\mathrm{s}}|^2 \delta(\hbar\omega - \hbar\omega_{\mathrm{s}}). \tag{6}$$

In the basis chosen, Eq. (5) takes the form

$$i\hbar \frac{\partial \rho_{nv,n'v'}(t)}{\partial t} = [H_S, \rho_S(t)]_{nv,n'v'} - i\hbar\gamma_0 (v + v') \rho_{nv,n'v'}/2 + i\hbar\gamma_0 \sqrt{v+1}\sqrt{v'+1}\, \rho_{n,v+1,n',v'+1}, \tag{7}$$

where the first term in the right side of Eq. (7) comes from the contribution of primary system Hamiltonian H_S, and second part comes from the first two terms in the second bracket on the right side of Eq. (5), and the last term involves energy transfer from the higher to the lower vibrational levels.[25] This equation will be solved numerically.

B. The semiclassical approximation

The dimensionless displacement of the single primary oscillator is approximated in the semiclassical approximation by

a time-dependent configuration $q(t) = \langle d_0^\dagger(t) + d_0(t)\rangle$ as[26,27]

$$q(t) = \frac{1}{\hbar}\int_0^t d\tau\, D^r(t-\tau)\alpha_2\langle c_2^\dagger(\tau)c_2(\tau)\rangle, \tag{8}$$

arising from the interaction among the electron, the active vibration and the phonon bath; here D^r is the retarded green function of the active vibration.

Equation (8) assumes that the displacement coordinate q responds to the average electron population (in the present calculation, on site 2). This is a mean field description akin to the Ehrenfest approximation that is to be tested in the calculations described below.

Using the wide-band approximation

$$D^r(\omega) = \frac{1}{\omega+\omega_0+i\gamma_0/2} - \frac{1}{\omega-\omega_0+i\gamma_0/2} \tag{9}$$

and its Fourier transform

$$D^r(t) = i[e^{(i\omega_0-\gamma_0/2)t} - e^{(-i\omega_0-\gamma_0/2)t}] = -2sin(\omega_0 t)e^{-\gamma_0 t/2}, \tag{10}$$

and substituting Eq. (10) into Eq. (8), we get

$$q(t) = -\frac{2}{\hbar}\int_0^t d\tau sin[\omega_0(t-\tau)]e^{-\gamma_0(t-\tau)/2}\alpha_2\langle c_2^\dagger(\tau)c_2(\tau)\rangle. \tag{11}$$

Here γ_0 has been defined in Eq. (6), and neglecting the real part of the vibration self-energy gives the solution for $q(t)$. Finally replacing $d_0^\dagger + d_0$ in the electron-vibration coupling Eq. (2) by $q(t)$ (Eq. (11)), we get the effective semiclassical electronic system Hamiltonian as[26,28,29]

$$H_{eff} = \sum_{l=0}^{4}\varepsilon_l c_l^\dagger c_l + V\sum_{l=0}^{3}(c_l^\dagger c_{l+1} + c_{l+1}^\dagger c_l) + F(t)c_2^\dagger c_2, \tag{12}$$

with[30]

$$F(t) = \alpha_2 q(t) = -\frac{2\alpha_2^2}{\hbar}\int_0^t d\tau sin[\omega_0(t-\tau)]e^{-\gamma_0(t-\tau)/2} \times \langle c_2^\dagger(\tau)c_2(\tau)\rangle. \tag{13}$$

The system density matrix ρ_S, which in this semiclassical approximation is derived from the Hamiltonian H_{eff} in Eq. (12), can be solved using the Liouville equation

$$i\hbar\frac{d\rho_S}{dt} = [H_{eff}, \rho_S]. \tag{14}$$

III. POPULATION DISTRIBUTION, POPULATION FORMATION TIME, AND ELECTRON-VIBRATION COUPLING ENERGY

The on-site electronic population at any time t is

$$P_l(t) = \langle c_l^\dagger(t)c_l(t)\rangle, \text{ with } \sum_{l=0}^{4} P_l(t) = 1. \tag{15}$$

Since the time-dependent values P_l oscillate, it is better to show these values using a coarse grained time-dependent average value

$$\bar{P}_l(t) = \frac{1}{2\Delta T}\int_{t-\Delta T}^{t+\Delta T} d\tau\, P_l(\tau). \tag{16}$$

Below we use $\Delta T = 50$ fs.

The population formation time in site 2 can be defined as the time point at which population P_2 reaches a certain value. Below, we shall define the "formation time" as the time at which the target population reaches $\sim(1 - e^{-1} \approx 0.76)$ of its final value.[31] Thus we use the criterion

$$\bar{P}_2(\tau_p) = P_2^\infty(1 - e^{-1}). \tag{17}$$

P_2^∞ is the time-averaged value of P_2 in the long time limit and τ_p is the population formation time.

The electron-vibration coupling energy E_P is

$$E_p = \begin{cases} \alpha_2\langle c_2^\dagger c_2(d_0^\dagger + d_0)\rangle, & \text{quantum approach,} \\ F(t)\langle c_2^\dagger c_2\rangle, & \text{semiclassical approach.} \end{cases} \tag{18}$$

Note that the semiclassical result is proportional to $\alpha_2^2\langle c_2^\dagger c_2\rangle^2$, in contrast to the quantum result.

IV. NUMERICAL CALCULATION

For the initial numerical simulation, we set $\varepsilon_l = 0$ for $l = 0, 1, 3, 4$ with $\varepsilon_2 = -0.2$ eV (ε_2 is lower than the other site energies), $V = 0.1$ eV, $v_{\max} = 9$, $\alpha_2 = 0.0707$ eV, $\omega_0 = 0.1$ eV, $\gamma_0 = 0.04$ eV. We will vary those parameters to examine more cases. All the results described below use the initial condition $c_n^\dagger c_n = \delta_{n,0}$ with a given site index n for the electronic state (in the calculations presented below $n = 0$), and $v = 0$ (ground vibrational level) for the primary phonon. For our purpose—comparing the quantum calculation and the mean-field semiclassical approximation—it is sufficient to consider the zero temperature case.

In the quantum approach, we need to set $v_{\max}$ large enough to assure convergence of the calculation. At $T = 0$ only vibrational damping takes place and the calculation converges at $v_{\max} = 3$ (see Fig. S1 in the supplementary

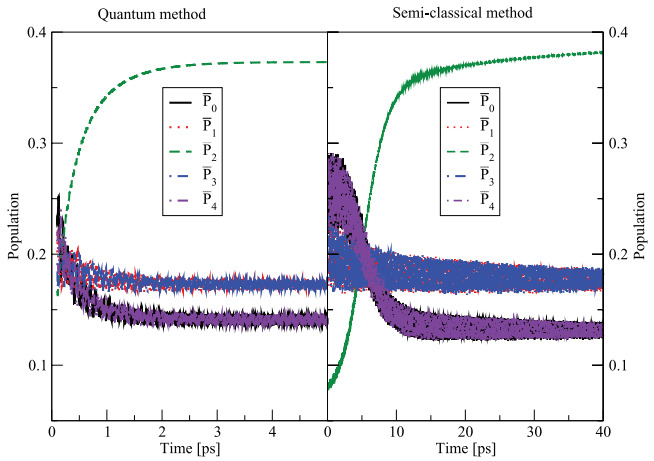

FIG. 2. Average population distribution on different sites l ($l = 0, 1, 2, 3, 4$) shown as a function of time starting from 0.05 ps. $\varepsilon_l = 0$ ($l = 0, 1, 3, 4$), $\varepsilon_2 = -0.2$ eV, $V = 0.1$ eV, $\alpha_l = 0$ ($l = 0, 1, 3, 4$), $\alpha_2 = 0.0707$ eV, $\hbar\omega_0 = 0.1$ eV, $\hbar\gamma_0 = 0.04$ eV. $\bar{P}_1 = \bar{P}_3$.

information[32]). At non-zero temperatures vibrational excitation is possible, and larger $\nu_{\max}$ will be needed.

V. POPULATION LOCALIZATION AND POLARON FORMATION

As noted above, the electron-vibration coupling is associated with transitions involving site 2 and the system is coupled to the bath through the single primary vibration. As shown in Fig. 2, for small V, much of the electron population will localize on site 2, forming a local polaron with large population. The quantum results (Sec. II) are shown on left panel and the semiclassical results (Sec. III) are displayed in the right panel. The respective results are qualitatively similar: $\bar{P}_2$ (polaron population) rises and saturates at values that are similar in both approaches. However, the rise time obtained from the quantum calculation is much shorter than its semiclassical counterpart: $\bar{P}_2$ reaches its maximum value at 2 ps in the quantum calculation, while in the semiclassical calculation it takes about 15 ps. This difference demonstrates the shortcoming of the semiclassical approximation, or rather—its reliance on the mean field approximation: The localizing phonon moves on a potential surface that is substantially different from what it actually experiences once the localization process has started. Figures 3(a) and 3(b) show time-dependent dynamics of those populations on a short time scale.

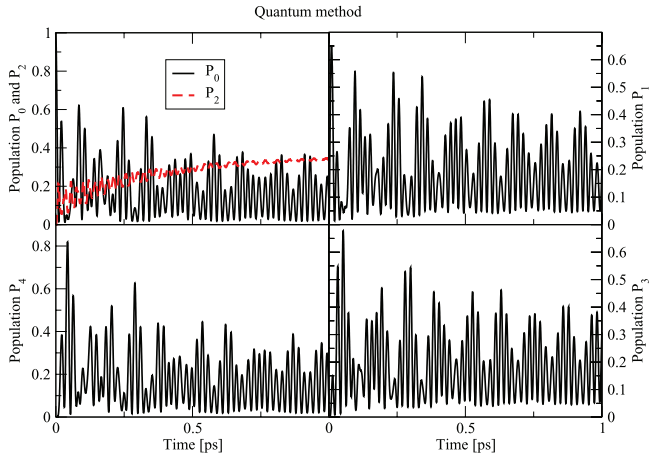

(a)

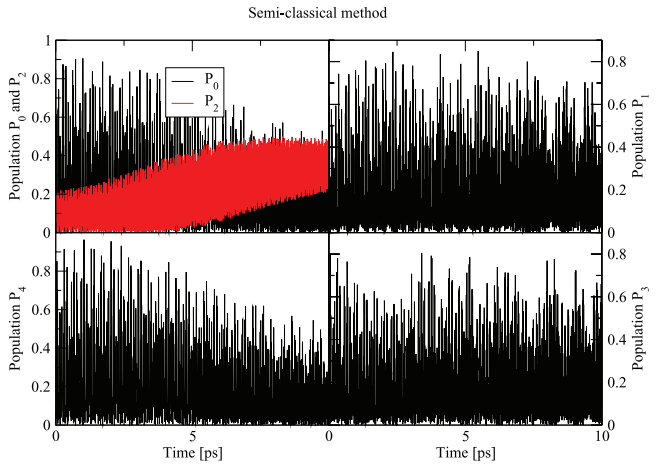

(b)

FIG. 3. Population distribution on different sites l ($l = 0, 1, 2, 3, 4$) shown as a function of time. $\varepsilon_l = 0$ ($l = 0, 1, 3, 4$), $\varepsilon_2 = -0.2$ eV, $V = 0.1$ eV, $\alpha_l = 0$ ($l = 0, 1, 3, 4$), $\alpha_2 = 0.0707$ eV, $\hbar\omega_0 = 0.1$ eV, $\hbar\gamma_0 = 0.04$ eV.

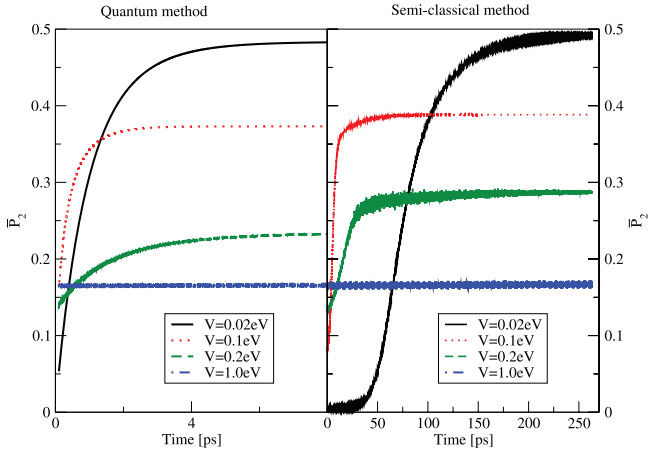

FIG. 4. Average population $\bar{P}_2$ as a function of time with different nearest neighbor tunneling parameter V. $\varepsilon_l = 0$ ($l = 0, 1, 3, 4$), $\varepsilon_2 = -0.2\,eV$, $\alpha_l = 0$ ($l = 0, 1, 3, 4$), $\alpha_2 = 0.0707$ eV, $\hbar\omega_0 = 0.1$ eV, $\hbar\gamma_0 = 0.04$ eV.

A. Influence of the tunneling amplitude *V*

The dynamics and extent of population localization is sensitive to the coupling V between nearest neighbor sites. For small V the coherent transfer between the different sites is weak and the population tends to localize, forming a polaron on site 2 whose coupling to the primary vibration results in a lower energy. For large V the population tends to equalize on neighboring sites, showing an oscillatory behavior (here only the average is shown). As shown in Fig. 4, the average population $\bar{P}_2$ on the impurity site decreases with increasing V, although the polaron is in principle formed on site 2. For $V = 1.0$ eV, delocalization dominates and the charge population rapidly reaches a uniform distribution. Recall that the

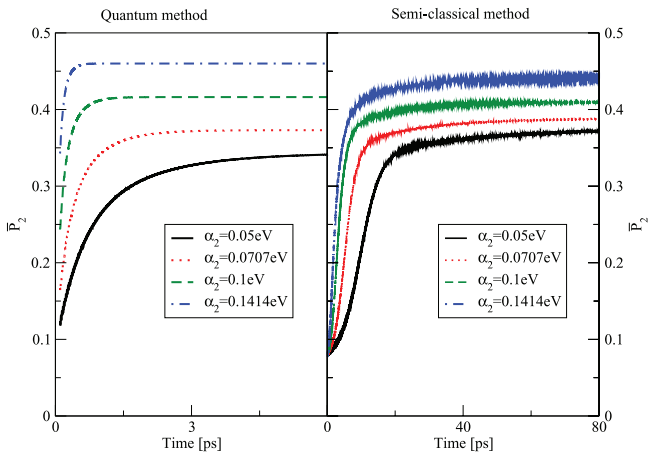

FIG. 5. Average population $\bar{P}_2$ shown as a function of time with different electron-vibration coupling parameter α_2. $\varepsilon_l = 0$ ($l = 0, 1, 3, 4$), $\varepsilon_2 = -0.2$ eV, $V = 0.1$ eV, $\alpha_l = 0$ ($l = 0, 1, 3, 4$), $\hbar\omega_0 = 0.1$ eV, $\hbar\gamma_0 = 0.04$ eV.

original small-polaron model of Holstein[33–38] was developed for narrow-band (small V) materials.

B. Effect of the electron-vibration coupling

The coupling strength α_2 between the electronic motion and the vibration at site 2 also affects the localization process. In the quantum method, electrons can evolve from the other sites to the vibronic states through this coupling as shown in the last term on the right side of Eq. (2). With larger α_2, more population will transfer and form a polaron with large population on the middle site. Qualitatively, similar evolution takes place in the semiclassical calculation, as seen in Eq. (13), and some population will be localized to form a polaron. As shown in Fig. 5, the population $\bar{P}_2$ in the steady state increases with this coupling strength. The more rapid population relaxation obtained in the quantum treatment occurs because in the quantum analysis, the actual population at site 2 is used, while in the semiclassical treatment, it is only the average population which drives the coupling.

In Figs. 6(a) and 6(b), P_2^{∞} (defined below Eq. (17)) is plotted in 3D changing the coupling V and the electron-phonon coupling α_2. With a small V, P_2^{∞} is around 0.5.[39] Choosing larger values of V decreases the site 2 population as can be expected, as shown in the corners of Figs. 6(a) and 6(b). However upon increasing α_2, the population builds up again; the polaron population value is mainly determined by the parameters V and α_2.

C. Comparison of population formation times

In Figs. 7(a) and 7(b) the population formation time is shown in 3D as a function of V and α_2. The formation time obtained by the semiclassical method is longer than the quantum method. The population formation time decreases with electron-phonon coupling α_2 but then saturates. It also decreases with coupling V, but there is a turnover in the quantum formation time beyond a $V \sim 0.1$ eV. This is due to the fact that for large V, the excitation relaxes into a delocalized population. The population distribution is roughly constant in this limit as shown in Fig. 4. The formation time should now be referred to simply as population relaxation time.

As shown in Figs. 6(a) and 6(b), with a larger value of V, the population on site 2 decreases, while by increasing the electron-phonon coupling strength α_2, the population builds up. The Hamiltonian parameters are selected to

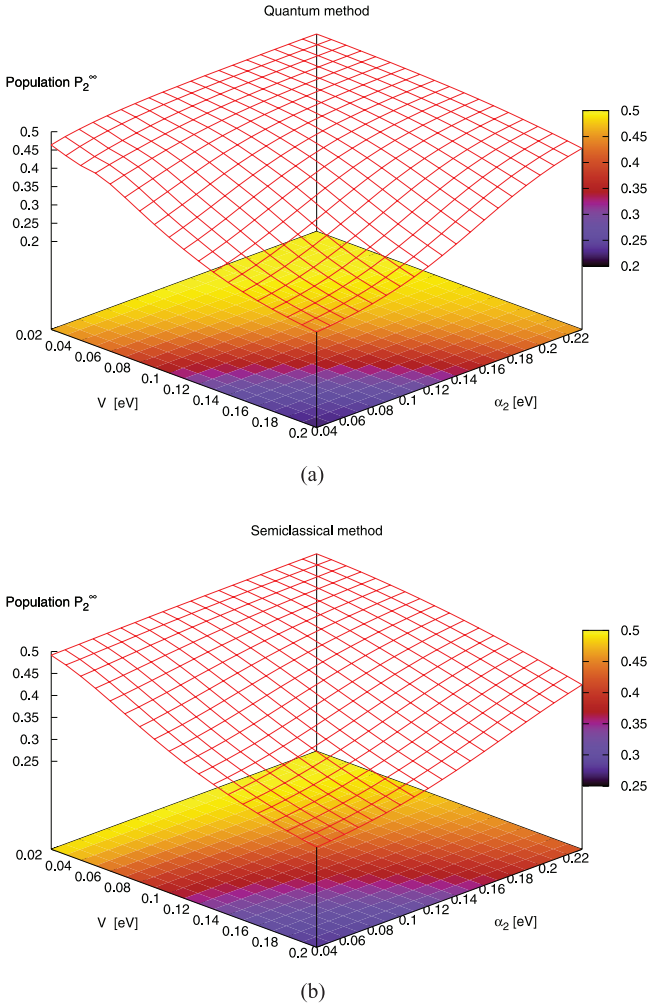

FIG. 6. P_2^{∞} (population on site 2 in the steady state) shown as a function of the nearest neighbor site coupling parameter V and electron-phonon coupling α_2. $\varepsilon_l = 0$ ($l = 0, 1, 3, 4$), $\varepsilon_2 = -0.2$ eV, $\hbar\omega_0 = 0.1$ eV, $\hbar\gamma_0 = 0.04$ eV. Quantum method used for panel (a) and semiclassical method used for (b).

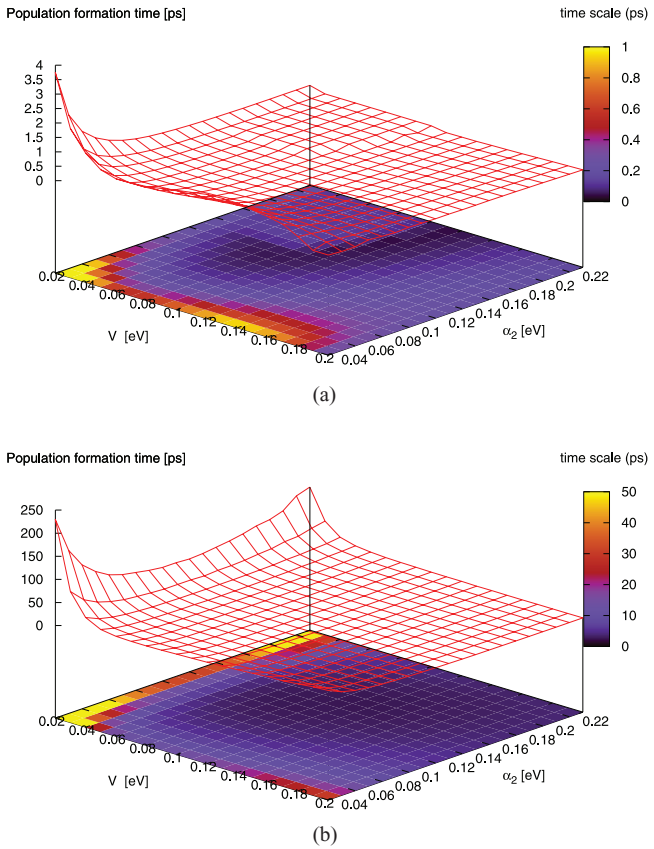

FIG. 7. Population formation time for P_2 shown as a function of the nearest neighbor site coupling parameter V and electron-phonon coupling α_2. $\varepsilon_l = 0$ ($l = 0, 1, 3, 4$), $\varepsilon_2 = -0.2$ eV, $\hbar\omega_0 = 0.1$ eV, $\hbar\gamma_0 = 0.04$ eV. Quantum method used for panel (a) and semiclassical method used for (b).

represent realistic values of V and electron-phonon coupling[28] encountered in real organic and inorganic systems. From Figs. 7(a) and 7(b) we see that the population formation time decreases with increasing V and α_2. It also decreases with increasing γ_0, which represents the coupling strength between the vibrations and the environment. Increasing the frequency ω_0 of the primary vibration, makes the relaxation process and the population formation time shorter. These four parameters V, α_2, γ_0, and ω_0 can work together to determine the population formation time.

D. The short time dynamics of polaron formation

In Fig. 8(a) we compare the time-dependent dynamic processes for P_2 and E_P (Eq. (18)). Both of them reach their steady state very quickly. When P_2 reaches its maximum, E_p is at minimum, and vice versa. This represents the damping of a coherent oscillator where displacement and population keep their phase delay throughout. The picture (Fig. 8(b)) is somewhat different in the semiclassical case, P_2 and F_2 are also delayed but we now see beats due to the interference of waves scattering from an oscillating potential. Both quantities reach their steady state more slowly in this case.

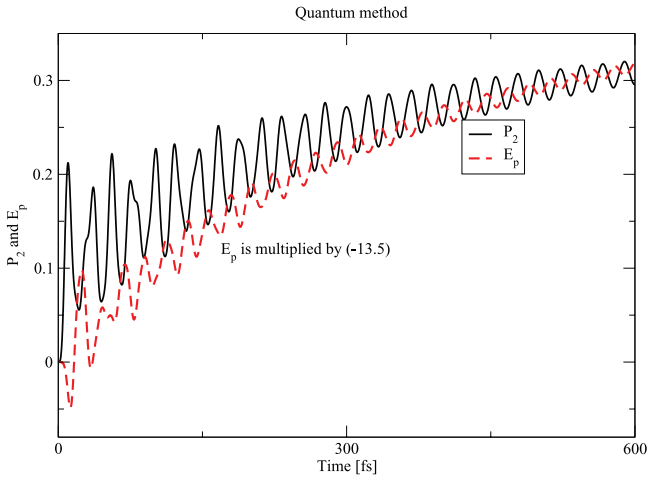

(a)

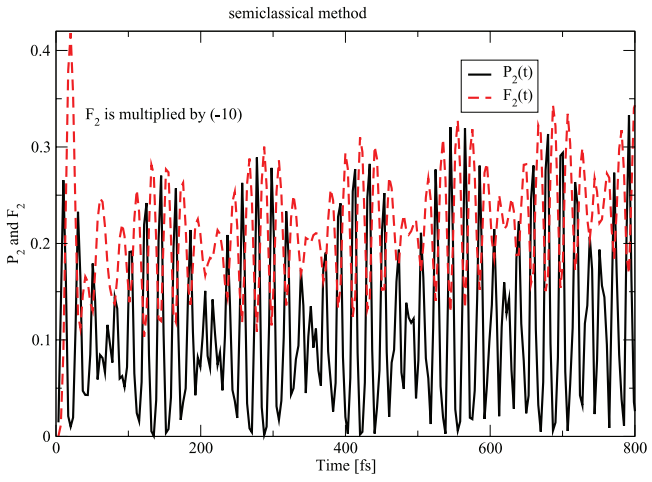

(b)

FIG. 8. (a) Population P_2 and electron-vibration coupling energy E_P are shown as a function of time; (b) Population P_2 and the electron-phonon coupling energy $F_2(t)$ are shown as a function of time. $\varepsilon_l = 0$ ($l = 0$, 1, 3, 4), $\varepsilon_2 = -0.2$ eV, $\alpha_l = 0$ ($l = 0$, 1, 3, 4), $\alpha_2 = 0.0707$ eV $\hbar\omega_0 = 0.1$ eV, $\hbar\gamma_0 = 0.04$ eV. Quantum method used for panel (a) and semiclassical method used for (b). The unit of E_P and F_2 is eV.

VI. CONCLUSION

In this paper we have compared fully quantum and semiclassical models for polaron formation. The latter is based on Ehrenfest dynamics for the calculation of the polaron formation process. We used a one-dimensional tight binding model that includes electron-phonon coupling at only one site, which acts as a polaron trap. Subsequent vibrational relaxation allows the system to relax into equilibrium. The results from both methods show qualitatively similar behavior, however with markedly different time scales: the population formation time obtained from the quantum calculation can be 10 times faster compared to the semiclassical method. This discrepancy becomes smaller with increasing intersite coupling V (for large V no localized polaron is formed) since the classical limit is reached for $V \gg \omega_0$.

The different relaxation times obtained in the quantum and the semiclassical calculations result from the use of mean field approximation in the latter. In this approximation, the primary oscillator responds to the average occupation of site 2 which effectively makes it move on a potential surface that is markedly different (less binding) than the one it experiences once localization is initiated. Localization on this average potential is slower. This averaging assumption may be justified when the electron motion is much faster than the vibration, that is, for large V ($V \gg \hbar\omega_0$). Another minor difference between the two calculations is the use of a master equation in the quantum calculation, and an essentially equivalent Langevin equation in the semiclassical one, to describe the relaxation of the primary phonon. These relaxation schemes are equivalent, provided that care is taken to use parameters that imply the same relaxation rate in both cases, as was done here.

The conclusion would also apply to the simulations of Kopidakis *et al.*[40] and the many other papers where the vibrations are also treated with semiclassical dynamics. It would seem that depending on electron bandwidth, the formation time is considerably overestimated in these works, perhaps by an order of magnitude or more. The semiclassical results are essentially in agreement with the conclusions reached by Emin and Kriman[41,42] using the Holstein diatomic polaron lattice model. These authors showed that population localization and polaron formation depend critically on the ratio of the tunneling energy V and the width of the Bloch phonon dispersion, which effectively plays the role of the dissipation term since outward traveling phonon Bloch waves will not return. Finally, it turns out in this model that the population on site 2 never exceeds 0.5 however small we make V. However, introducing a small electron phonon coupling on the other sites in the chain allows the system to reach the true ground state and the population on site 2 can now climb up to 1. This interesting observation should be investigated in detail, particularly at finite temperature.

ACKNOWLEDGMENTS

This work was supported by the Non-Equilibrium Energy Research Center (NERC) which is an Energy Frontier Research Center funded by the U.S. Department of Energy, Office of Science, Office of Basic Energy Sciences under Award No. DE-SC0000989. M.R. thanks the chemistry division of the NSF (CHE-1058896) for support. The research of A.N. is supported by the Israel Science Foundation Grant No. 164608, the U.S.-Israel Binational Science Foundation, and the European Research Council under the European Union's Seventh Framework Program (FP7/2007-2013; ERC Grant agreement No. 226628). The authors would like to thank Boris D. Fainberg for his insightful remarks.

[1]R. A. Marcus and N. Sutin, Biochim. Biophys. Acta **811**, 265 (1985).
[2]P. F. Barbara, T. J. Meyer, and M. A. Ratner, J. Phys. Chem. **100**, 13148 (1996).
[3]M. Bixon and J. Jortner, Adv. Chem. Phys. **106**, 35 (1999).
[4]Y. A. Berlin, I. V. Kurnikov, D. Beratan, M. A. Ratner, and A. L. Burin, Top. Curr. Chem. **237**, 1 (2004).
[5]S. S. Skourtis, D. H. Waldeck, and D. N. Beratan, Annu. Rev. Phys. Chem. **61**, 461 (2010).
[6]R. A. Marcus, J. Chem. Phys. **24**, 966 (1956).
[7]B. Kippelen and J. L. Brédas, Energy Environ. Sci. **2**, 251 (2009).
[8]S. Gunes, H. Neugebauer, and N. S. Sariciftci, Chem. Rev. **107**, 1324 (2007).
[9]J. D. Servaites, S. Yeganeh, M. A. Ratner, and T. J. Marks, Adv. Funct. Mater. **20**, 97 (2010).
[10]A. Aviram and M. A. Ratner, Chem. Phys. Lett. **29**, 277 (1974).
[11]C. Joachim and M. A. Ratner, Nanotechnology **15**, 1065 (2004).
[12]A. Nitzan and M. A. Ratner, Science **300**, 1384 (2003).
[13]A. Nitzan, *Chemical Dynamics in Condensed Phases* (Oxford University Press, Oxford, 2006).
[14]A. P. Horsfield, D. R. Bowler, A. J. Fisher, T. N. Todorov, and M. J. Montgomery, J. Phys.: Condens. Matter **16**, 3609 (2004).
[15]J. C. Cuevas and E. Scheer, *Molecular Electronics: An Introduction to Theory and Experiment* (World Scientific, New Jersey, 2010).
[16]*Introduction to Molecular Electronics*, edited by M. C. Petty, M. R. Bryce, and D. Bloor (Oxford University Press, New York, 1995).
[17]R. Gerber and M. Ratner, J. Phys. Chem. **92**, 3252 (1988).
[18]M. Einax, M. Dierl, and A. Nitzan, J. Phys. Chem. C **115**, 21396 (2011).
[19]G.-Q. Li, A. Nitzan, and M. A. Ratner, Phys. Chem. Chem. Phys. **14**, 14270 (2012).
[20]P. Szymanski, S. Garrett-Roe, and C. B. Harris, Prog. Surf. Sci. **78**, 1 (2005).
[21]L. Turi, W. S. Sheu, and P. J. Rossky, Science **309**, 914 (2005).
[22]O. V. Prezhdo and P. J. Rossky, J. Chem. Phys. **107**, 825 (1997).
[23]J. C. Tully, J. Chem. Phys. **93**, 1061 (1990).
[24]J. Bonča and S. A. Trugman, Phys. Rev. Lett. **75**, 2566 (1995).
[25]Because of the zero temperature and Bose-Einstein distribution function $N_B(\omega) = \frac{1}{e^{\hbar\omega/KT}-1} \equiv 0$ (except for the ground vibrational level), the energy transfer only happens from the higher levels to its nearest lower level. For non-zero temperature, there will be transfer from lower to higher levels.
[26]M. Galperin, M. A. Ratner, and A. Nitzan, Nano Lett. **5**, 125 (2005).
[27]G.-Q. Li, B. Movaghar, and M. A. Ratner, "Dynamic electron localisation initiated by particle-bath coupling," Phys. Rev. B (submitted).
[28]V. D. Lakhno, Phys. Chem. Chem. Phys. **4**, 2246 (2002).
[29]V. D. Lakhno, J. Biol. Phys. **31**, 145 (2005).
[30]Note that the last term in Eq. (12) is proportional to $\langle c_2^\dagger c_2\rangle \bullet c_2^\dagger c_2$. This is an artifact of the semiclassical approach.
[31]F. D. Lewis, H. H. Zhu, P. Daublain, T. Fiebig, M. Raytchev, Q. Wang, and V. Shafirovich, J. Am. Chem. Soc. **128**, 791 (2006).
[32]See supplementary material at http://dx.doi.org/10.1063/1.4776230 for more details about the electron-vibration coupling energy $F(t)$ and the influence of the vibration-phonon relaxation to the polaron formation process.
[33]T. Holstein, Ann. Phys. **8**, 325 (1959).
[34]D. Emin, Adv. Phys. **22**, 57 (1973).
[35]D. Emin, *Polarons* (University Press, Cambridge, 2012).
[36]Y. A. Firsov, *Polarons* (Nauka, Moscow, 1975).
[37]G. L. Sewell, *Polarons and Excitons* (Plenum, New York, 1963).
[38]D. Golež, J. Bonča, L. Vidmar, and S. A. Trugman, Phys. Rev. Lett. **109**, 236402 (2012).
[39]Note that localization with more than 0.5 population on site 2 can indeed be achieved by allowing each site to be coupled to its own vibronic oscillator, even if these couplings constant are much weaker compared to site 2. This analysis, to be developed further in future, leads to the tentative conclusion that the "true equilibrium distribution," within the model itself, may not always be reached with oversimplified models. This question, namely under what circumstances can the system reach the true ground state (or excited state at finite temperature T) is an interesting one.
[40]G. Kopidakis, C. M. Soukoulis, and E. N. Economou, Phys. Rev. B **51**, 15038 (1995).
[41]D. Emin and A. M. Kriman, Phys. Rev. B **34**, 7278–7289 (1986).
[42]D. Emin, Monatsch. Chem. **144**, 3–10 (2012).